Journal of Computers Vol. 32 No. 3, 2021, pp. 237-248
doi:10.3966/199115992021063203017

Double Rotation Representation and Attitude Algorithm of Spinning Bodies

Shuang-biao Zhang[1*], Jia-qi Yu[2]

[1] School of Information Communication Engineering, Beijing Information Science and Technology University, 100101, Beijing, China
zhang_shb@bistu.edu.cn

[2] Beijing Institute of Control and Electronic Technology, 100038, Beijing, China
yujq2004@163.com

Received 17 April 2021; Revised 1 May 2021; Accepted 17 May 2021

Abstract. Self-spin bodies have the disunification problem of flight movement and rotation representation that could induce attitude algorithms to generate attitude error. To address this problem, a double rotation representation is proposed in this paper and the cone angles are defined between the reference frame and the body frame. Then, the angular model based on the double rotation process is derived in detail for flight control, and an attitude algorithm with the rotation vector and the angle conversion for navigation are also provided. Simulation results show that the varying cone speed has a bigger effect than the varying half cone angle, and the double rotation representation can decouple the coning motion completely and has better accuracy than the three rotation representation. Moreover, a good resistance of the attitude algorithm with rotation vector against the varying coning motion is shown though the non-commutative error still exists.

Keywords: self-spin body, rotation representation, attitude error, decoupling

1 Introduction

1.1 Background

Many flying bodies like guided rockets, bullets and shells are designed purposely to perform flight motion with high self-spin speed, which is seen as a significant way for flying weapons to guarantee the reduction of drop point area and the simplification of control systems [1]. As the variant self-spin weapons flourishing, a trend of increasing spinning speed of bodies is rising based on the analysis of lateral cases [2-3].

Attitude algorithm is key for flight bodies as its accuracy determines the flight stability and navigation and control accuracy. However, a fact that self-spin flight bodies have different features other than normal non-self-spin ones and fast diverging algorithm error generated is taken into account seriously by the associated researchers. Self spinning, pitching and yawing make self-spin flight bodies experience a complex angular vibration with varying frequency if extracted from a quite short period of the whole flight. This kind of vibration is firmly reckoned as a nonnegligible effect, because it would result in signal-circle motions and sometimes even double-circle motions called coning motion and induce normal attitude algorithms to generate diverging error [4-5]. Therefore, in order to maintain the superiority of self-spinning mode and restrain algorithm error, many researchers dedicate themselves into uncovering the principle and weakening the angular vibration effect.

* Corresponding Author

1.2 Related Work

Commonly, the three rotation representation defines the rotation relationship by rotating around three different axes successively and using three attitude angles between the body frame and the reference frame [6]. Fig. 1 shows the detailed rotation process and the attitude angles, where ψ is the yaw angle, ϑ is the pitch angle and γ is the roll angle. The rotation and attitude angles are independent so that they may occur in any combination, like singly, in pairs or overall.

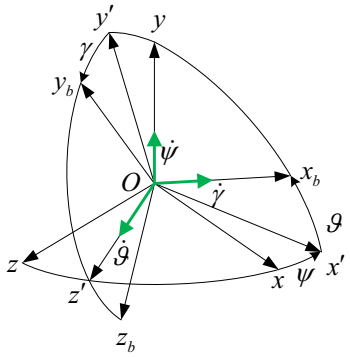

Fig. 1. Three rotation representation

For non-self-spin bodies, a slight rolling motion is performed generally to cooperate other two motions to make a turn or cruise, which means it does not exist all the time. The angular vibration just seems like a disturbance but could not evolve into a persistent coning motion, so the control and navigation systems use three rotation representation to describe attitude angles of flying bodies all right.

But, if the self-spin motion is added, the real process changes and becomes quite different. The first reason is the disunification of flight movement and rotation representation. It is assumed that a non-spin body performs a shortly existing coning motion with the cone speed Ω for some reason. The roll angle is supposed to be zero all the time wherever the x axis swings, as is shown in Fig. 2(a). This process could be decoupled into pitch and yaw motions using three-axis rotation representation, and it could also be seen that the x_b axis swings around the point O. If a self-spin motion is added to make the body become self-spin, the roll angle begins varying, as is shown in Fig. 2(b). By this time, the existence of self-spin motion has actually made the whole angular motion coupled and changed the rotation process of a self-spin body from the three-rotation mode to the two-rotation, and then the algorithm error is generated. The other reason comes from the approximation of rotation vector. Conventional attitude algorithms use rotation vector method to update attitude matrix, but the cross-product term of rotation vectors is hard to calculate and often ignored by using the data directly from gyroscopes. This kind of attitude approximation error is called non-commutative error and accumulates during each iterative updating. More importantly, coning motion would aggravate the non-commutative error effect and make it mixed with the coning error.

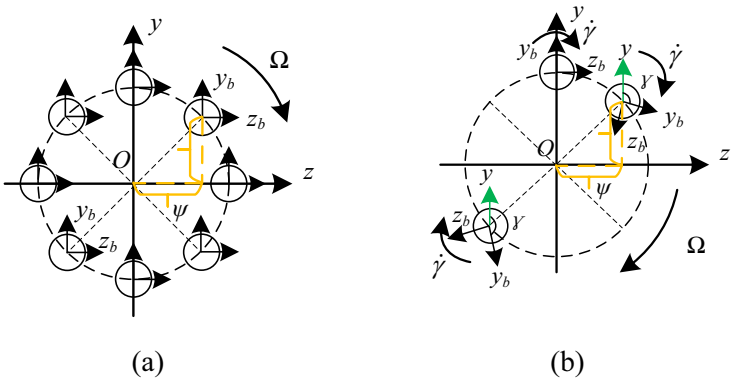

Fig. 2. Coning motion presented by the three rotation representation

Meanwhile, many works based on the three rotation representation focus on how to restrain the angle errors by increasing the subsamples of rotation vector and shortening the updating time of attitude algorithms. The concept of optimizing attitude algorithm coefficients is first proposed by Miller to restrain attitude errors indued by coning environment, and this kind of algorithms is called conic error compensation [7]. From then on, two-subsample, three-subsample, four-subsample algorithms are exploited to decrease error diverging rate, and the algorithm accuracy is increased with the number of subsamples [8-10]. In fact, these works are trying to use the angular increment to calculate the rotation vector and regard the cross-product terms non-determined or ignored as the conic error, so the approaches to estimate the terms are worthy. Moreover, improving the attitude updating structure can maintain the real-time capability of algorithms, with the hardware performance allowing [11]. Reconstructing attitude is a new idea to use functional iteration of the Rodrigues vector and isolate the effect of angular coning motion [12]. All the works above need to transmit the rotation vector into the attitude angles with the three rotation representation, and they have analyzed the non-communicative error and supplied conservative ways to balance the attitude angle errors.

This is a notable reason that the discrepancy results in the problem of attitude error diverging and attracts many researchers to try to find valid solutions. However, an in-depth research from this respect has not been paid enough attention and carried out up to now. Therefore, the motivation of this paper is to demonstrate the rotational difference and continue working on solving algorithm error fast diverging problem. Moreover, the contribution of this paper is to present a double rotation representation for the angular motion to restrain the disunification of flight movement and rotation representation, derive an attitude algorithm for flight control in details and provide attitude update process for navigation.

The paper is organized as follows: Section 2 describes the double rotation representation. Section 3 provides the attitude update methods for attitude control and navigation. The simulation and analysis are shown in Section 4. In Section 5, the conclusion is given and the future work is presented.

2 Double Rotation Representation

2.1 Feature of Coning Motion

The self-spin motion for self-spin bodies is the very first motion since the time they start working, and then other angular motions come about and are subjoined onto the self-spin, so this successive process forms angular vibration and becomes the real flight motion of self-spin bodies. It is explicit and logical, but also shows that the angular vibration takes place with three rotations around two axes of a three-dimension coordinate system, where one is the self-spin axis and the other is the rotating axis of angular vibration. Clearly, it is a discrepancy and different from the three rotation representation.

In fact, coning motion is derived from gyroscopic effect. A self-spin body with the speed ω_0 would perform the cone swing motion with the precession speed Ω and the half cone angle α if it is disturbed by a lateral moment of force, as is shown in Fig. 3. During this process, the self-spin motion takes place firstly, and the cone swing motion made up by precession and nutation comes about after that. From Fig. 3, the two motions rotate x_b axis and x axis respectively, which would be coincident when the half cone angle α is zero. So, the coning motion is actually seen as a double rotation mode.

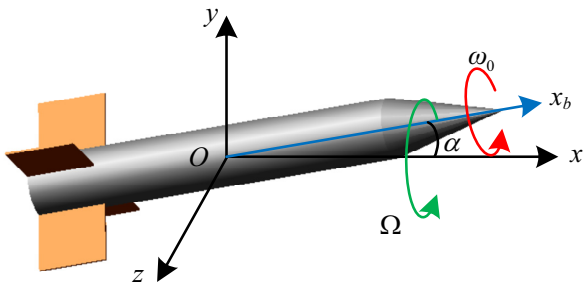

Fig. 3. Coning motion of self-spin bodies

2.2 Cone Frame and Cone Attitude

The cone frame $Oxyz$ is a reference frame used to describe the self-spin bodies of performing coning motion, and it is coincident with the body frame $Ox_by_bz_b$ through rotating around x, z' and x'_b sequentially. Thus, the precession angle δ_1 is defined by the first rotation, the nutation angle δ_2 is defined by the second rotation, and the roll angle δ_3 is defined by the last rotation. It is necessary to notice that the third rotation around x'_b axis is like the first rotation around x axis, so it has the effect of stacking rotation. In other words, the third rotation is dependent to the precession. So, the roll angle δ_3 is defined with respect to the precession. The rotation process is expressed as follows:

$$Oxyz \xrightarrow[x]{\dot{\delta}_1} Ox'y'z' \xrightarrow[z']{\dot{\delta}_2} Ox'_by'_bz'_b \xrightarrow[x'_b]{\dot{\delta}_3-\dot{\delta}_1} Ox_by_bz_b$$

where $\dot{\delta}_1$, $\dot{\delta}_2$, $\dot{\delta}_3$ are corresponding angular speeds. Based on the analysis above, the rotation process from the reference frame to the body frame is shown in Fig. 4.

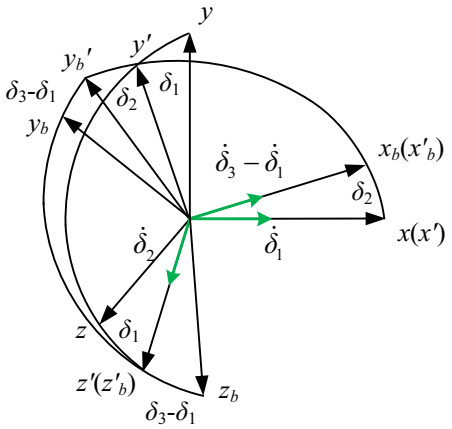

Fig. 4. Rotation process from the reference frame to the body frame

To explore the difference, the same example in Fig. 2 is reused here and the coning motion is described with the cone angles of the double rotation representation in Fig. 5. In Fig. 5(a), the fake roll angle is equal to the precession angle even though no active self-spin motion exists. In Fig. 5(b), the fake roll angle is equal to the sum of the precession angle and the real roll angle. This is the reason why the rolling motion needs to isolate the precession.

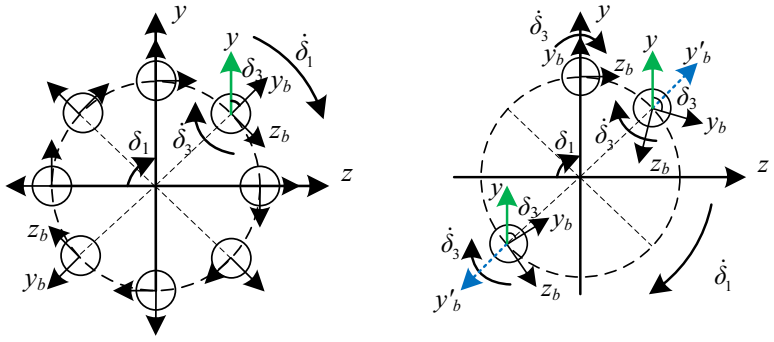

(a) No active self-spin motion (b) Active self-spin motion

Fig. 5. Coning motion presented by the double rotation representation

3 Attitude Updating Methods

3.1 Attitude Updating for Flight Control

Attitude determination is a key step of flight control, and acquiring attitude data is to use angular velocity to update attitude based on the angular model of the rotation process for control systems and monitor the body in the right trajectory. In this paper, a cone angular model for self-spin bodies is derived in detailed.

Through the first rotation based on Fig. 4, the transfer matrix C_1 is determined as:

$$C_1 = \begin{bmatrix} 1 & 0 & 0 \\ 0 & \cos\delta_1 & \sin\delta_1 \\ 0 & -\sin\delta_1 & \cos\delta_1 \end{bmatrix} \tag{1}$$

Through the second rotation, the transfer matrix C_2 is determined as:

$$C_2 = \begin{bmatrix} \cos\delta_1 & \sin\delta_1 & 0 \\ -\sin\delta_1 & \cos\delta_1 & 0 \\ 0 & 0 & 1 \end{bmatrix} \tag{2}$$

Through the third rotation, the transfer matrix C_3 is determined as:

$$C_3 = \begin{bmatrix} 1 & 0 & 0 \\ 0 & \cos(\delta_3 - \delta_1) & \sin(\delta_3 - \delta_1) \\ 0 & -\sin(\delta_3 - \delta_1) & \cos(\delta_3 - \delta_1) \end{bmatrix} \tag{3}$$

Then, the transform matrix from the reference frame to the body frame is obtained:

$$C_c^b = C_3 C_2 C_1 \tag{4}$$

On the other hand, based on the transfer relationship, the angular velocity of the body frame with respect to the reference frame is established:

$$\boldsymbol{\omega} = C_3 C_2 C_1 \dot{\delta}_1 + C_3 C_2 \dot{\delta}_2 + C_3 (\dot{\delta}_3 - \dot{\delta}_1) \tag{5}$$

In fact, according to Fig. 4, each rotation rate can be projected and constitutes the angular velocity, so the first term can omit C_1, the second term can omit C_2 and the last term can omit C_3. Expanding (5), the angular velocity is described by:

$$\begin{bmatrix} \omega_x \\ \omega_y \\ \omega_z \end{bmatrix} = \begin{bmatrix} \dot{\delta}_1 (\cos\delta_2 - 1) + \dot{\delta}_3 \\ -\dot{\delta}_1 \cos(\delta_1 - \delta_3)\sin\delta_2 - \dot{\delta}_2 \sin(\delta_1 - \delta_3) \\ -\dot{\delta}_1 \sin(\delta_1 - \delta_3)\sin\delta_2 + \dot{\delta}_2 \cos(\delta_1 - \delta_3) \end{bmatrix} \tag{6}$$

where ω_x, ω_y, ω_z are the elements of the angular velocity. This is the angular model and it also could be degraded into the classical coning motion. By transforming (6), the differential equation of cone angles is obtained:

$$\begin{bmatrix} \dot{\delta}_1 \\ \dot{\delta}_2 \\ \dot{\delta}_3 \end{bmatrix} = \begin{bmatrix} 0 & \dfrac{\cos(\delta_1 - \delta_3)}{\sin\delta_2} & \dfrac{\sin(\delta_1 - \delta_3)}{\sin\delta_2} \\ 0 & -\sin(\delta_1 - \delta_3) & \cos(\delta_1 - \delta_3) \\ 1 & -\cos(\delta_1 - \delta_3)\tan\dfrac{\delta_2}{2} & -\sin(\delta_1 - \delta_3)\tan\dfrac{\delta_2}{2} \end{bmatrix} \begin{bmatrix} \omega_x \\ \omega_y \\ \omega_z \end{bmatrix} \tag{7}$$

It is clear that the cone angles can be updated as long as the nutation angle is unequal to zero.

3.2 Attitude Updating for Navigation

Attitude updating for navigation is used to determine acquire the attitude matrix, which differs from that for flight control, but the attitude can be calculated using the attitude matrix and provided for integrated systems of navigation and control. Normally, the rotation vector is also the popular method that uses angular velocity from gyroscopes to calculate the angular increment:

$$\boldsymbol{\phi}_l = \boldsymbol{a}_l + \delta\boldsymbol{\phi}_l \tag{8}$$

$$\boldsymbol{\phi}_l = \int_{t-1}^{t} \boldsymbol{\omega} \cdot dt \tag{9}$$

$$\delta\boldsymbol{\phi}_l \approx \int_{t-1}^{t} \left(\frac{1}{2}\boldsymbol{\phi}_l \times \boldsymbol{\omega} + \frac{1}{12}\boldsymbol{\phi}_l \times \left(\boldsymbol{\phi}_l \times \boldsymbol{\omega}\right) \right) dt \tag{10}$$

where l represents the lth calculation. According to (10), two cross-product terms are the non-commutative error and hard to calculated directly through integrating the angular velocity from gyroscopes, so they must be approximated by:

$$\delta\boldsymbol{\phi}_l = \sum_{i=1}^{N-1} \sum_{j=i+1}^{N} k_{ij} \Delta\boldsymbol{\phi}_l(i) \times \Delta\boldsymbol{\phi}_l(j) \tag{11}$$

where k_{ij} is the coefficients needed to be optimized, N represents the number of subsamples.

Using the rotation vector in (8), the attitude matrix can be updated:

$$C_{b(l)}^{c(l)} = C_{b(l-1)}^{c(l)} \cdot C_{b(l)}^{b(l-1)} \tag{12}$$

$$C_{b(l)}^{b(l-1)} = I + f_1(\boldsymbol{\phi}_l)(\boldsymbol{\phi}_l \times) + f_2(\boldsymbol{\phi}_l)(\boldsymbol{\phi}_l \times)^2 \tag{13}$$

$$f_1(\phi_l) = \frac{\sin|\boldsymbol{\phi}_l|}{|\boldsymbol{\phi}_l|} = \sum_{k=1} (-1)^{k-1} \frac{|\boldsymbol{\phi}_l|^{2(k-1)}}{(2k-1)!} \tag{14}$$

$$f_2(\boldsymbol{\phi}_l) = \frac{1-\cos|\boldsymbol{\phi}_l|}{|\boldsymbol{\phi}_l|^2} = \sum_{k=1} (-1)^{k-1} \frac{|\boldsymbol{\phi}_l|^{2(k-1)}}{(2k)!} \tag{15}$$

$$\boldsymbol{\phi}_l \times = \begin{bmatrix} 0 & -\phi_z & \phi_y \\ \phi_z & 0 & -\phi_x \\ -\phi_y & \phi_x & 0 \end{bmatrix} \tag{16}$$

Note that (12) is the transposition of (4) and is presented in detailed by:

$$C_b^c = \begin{bmatrix} C_{11} & C_{12} & C_{13} \\ C_{21} & C_{22} & C_{23} \\ C_{31} & C_{32} & C_{33} \end{bmatrix} \tag{17}$$

where $C_{11} = \cos\delta_2$, $C_{12} = -\cos(\delta_1 - \delta_3)\sin\delta_2$, $C_{13} = -\sin(\delta_1 - \delta_3)\sin\delta_2$, $C_{21} = \cos\delta_1\sin\delta_2$,

$C_{22} = \sin(\delta_1 - \delta_3)\sin\delta_1 + \cos(\delta_1 - \delta_3)\cos\delta_1\cos\delta_2$, $C_{23} = -\cos(\delta_1 - \delta_3)\sin\delta_1 + \sin(\delta_1 - \delta_3)\cos\delta_1\cos\delta_2$,

$C_{31} = \sin\delta_1\sin\delta_2$, $C_{32} = -\sin(\delta_1 - \delta_3)\cos\delta_1 + \cos(\delta_1 - \delta_3)\cos\delta_1\sin\delta_2$,

$C_{33} = \cos(\delta_1 - \delta_3)\cos\delta_1 + \sin(\delta_1 - \delta_3)\cos\delta_1\sin\delta_2$.

Then, the cone angles are determined by:

$$\hat{\delta}_1 = \arctan\frac{C_{31}}{C_{21}} \tag{18}$$

$$\delta_2 = \arccos C_{11} \tag{19}$$

$$\delta_1 - \hat{\delta}_3 = \arctan\frac{C_{13}}{C_{12}} \tag{20}$$

It needs to notice that (18) and (20) are the fake values, so the real ones should be determined according to Table 1 and Table 2.

Table 1. Real value of δ_1

C_{21}	C_{31}	δ_1
+	+	$\hat{\delta}_1$
-	-	$\hat{\delta}_1+\pi$
-	+	$\hat{\delta}_1+\pi$
+	-	$\hat{\delta}_1+2\pi$

Table 2. Real value of δ_3

C_{12}	C_{13}	δ_3
+	+	$\delta_1+\hat{\delta}_3$
+	-	$\delta_1+(\hat{\delta}_3+\pi)$
-	-	$\delta_1+(\hat{\delta}_3+\pi)$
-	+	$\delta_1+(\hat{\delta}_3+2\pi)$

3.3 Angle Conversion

Since the coning motion can be described by the two kinds of representation, the geometrical relationship between the double rotation representation and the three rotation representation can be set up, as shown in Fig. 6.

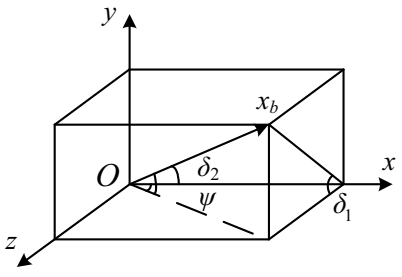

Fig. 6. Geometrical relationship between the double rotation representation and the three rotation representation

According to Fig. 6, the pitch angle and yaw angle can be calculated by:

$$\vartheta = \pm\arcsin\left|\sin\delta_1 \sin\delta_2\right| \tag{21}$$

$$\psi = \pm \arcsin \sqrt{\frac{\sin^2 \delta_2 - \sin^2 \vartheta}{\cos^2 \vartheta}} \tag{22}$$

Then, the sign of angles can be determined according to Table 3 and Table 4.

Table 3. Sign of Pitch Angle

δ_1	ϑ
[0° 180°]	+
(180° 360°]	−

Table 4. Sign of Yaw Angle

δ_1	ψ
[0° 90°) ∪ (270° 360°]	+
[90° 270°]	−

4 Simulation and Analysis

The classical coning environment is most used to test attitude algorithms. One reason is setting the coning environment conditions easily, and the other is demonstrating the validity of methods clearly. Thus, the double rotation representation and three rotation representation can be input the same conditions and examined which one can decouple the coning motion correctly and provide the accurate value. Meanwhile, the half cone angle and the spin angle are selected as the evaluation indexes in this paper. This is because the first angle can be composed and decomposed with the pitch angle and the yaw angle, and the second angle can be examined and compared to the self-spin process designed ahead. Therefore, based on the two evaluation indexes, simulations are made below.

4.1 Simulation for Attitude Algorithm of Flight Control

In the first simulation, it is assumed that the rolling and the precession have the same speed. Clearly, it is a scenario more likely a gyroscope calibration test where the sensitive axis of gyroscope is misalignment with the spinning axis of the calibration platform. Besides, the initial half cone angle is set to be zero, but it is varying with a rate 1.146 degrees per second, and the initial roll angle is 30 degrees. Table 5 shows the details of initial condition of simulation 1. So, the real roll angle and the half cone angle can be expected easily according to the condition.

Table 5. Initial Condition of Simulation 1

Parameters	Value
Roll angle	0°
Half cone angle	0°
Cone speed	360°/s
Rolling speed	360°/s
Rate of half cone angle	1.146°/s

From Fig. 7, the roll angle error and the half cone angle error by the double rotation representation for flight control are nearly zero but those by the three rotation representation are vibrating and diverging fast with time, which is seen from the red envelope lines. The vibrating error between the envelope lines can be seen as the coupled attitude error, which shows the disunification of the coning motion and the three rotation representation.

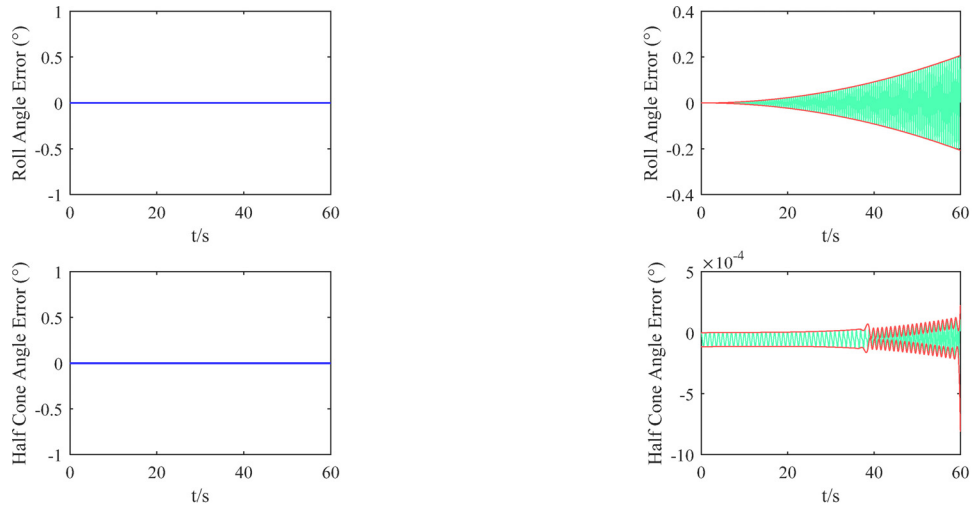

(a) Double Rotation Representation (b) Three Rotation Representation

Fig. 7. The roll angle error and the half cone angle error in Simulation 1

In the second simulation, the rolling speed and the precession speed are set to accelerate uniformly without changing other conditions. The details of initial condition of simulation 2 is shown in Table 6.

Table 6. Initial condition of simulation 1

Parameters	Value
Roll angle	0°
Half cone angle	0°
Cone speed	360°/s
Rolling speed	360°/s
Rate of half cone angle	1.146°/s
Rolling accelerator	24°/s^2
Precession accelerator	24°/s^2

The result is shown in Fig. 8. Comparing it with Fig. 8, the amplitude of the roll angle error remains unchanged, but the half cone angle error becomes bigger. It means varying coning motion has a big effect on the three rotation representation other than the double rotation representation during flight control.

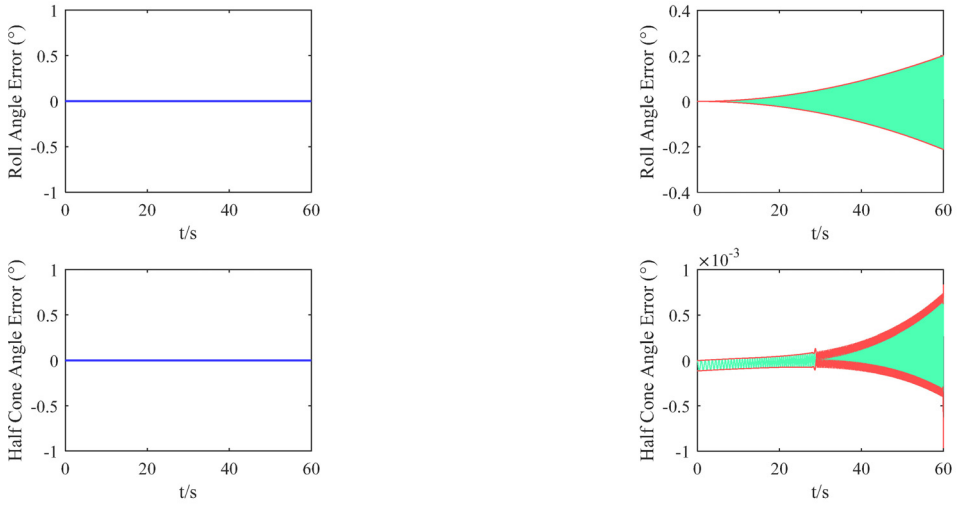

(a) Double Rotation Representation (b) Three Rotation Representation

Fig. 8. The roll angle error and the half cone angle error in Simulation 2

4.2 Simulation for Attitude Algorithm of Navigation

The attitude algorithm of navigation usually uses the rotation vector to update attitude. In this section, the simulations use the same input conditions respectively as the above two does. So, the simulation 3 is set to have the first simulation condition according to Table 5 and the simulation 4 is set to have the second simulation condition according to Table 6. Table 7 provides the coefficients of rotation vector updating [13].

Table 7. Coefficients of rotation vector updating

Coefficients	Value
k_{11}	0.45
k_{12}	0.675
k_{112}	-1.2229
k_{212}	1.0021
k_{312}	0.0396
k_{123}	-0.3771
k_{223}	1.2354
k_{323}	-0.3396
k_{113}	1.1562
k_{213}	-0.7625
k_{313}	0.0000

Fig. 9 and Fig. 10 show that the double rotation representation by the rotation vector also generates algorithm errors. This more likely means the error is the non-commutative error coming from the rotation vector, though it is still more accurate than the three rotation representation. Meanwhile, through comparing their envelope lines with those in Fig. 7 and Fig. 8, the rotation vector method by three rotation representation is found to have good resistance against the varying coning motion but the diverging effect of vibrating error does not seems improving.

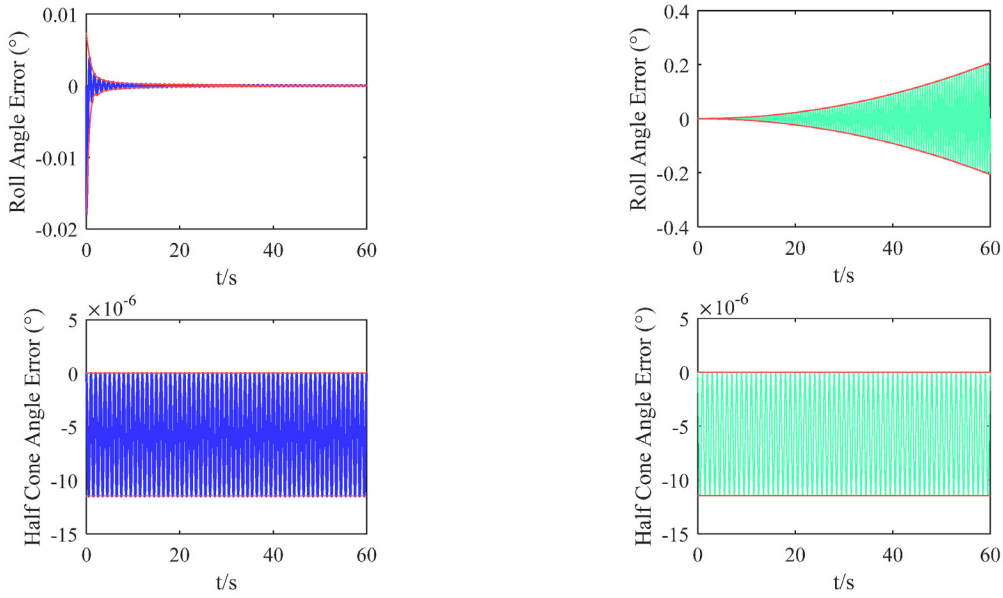

(a) Double Rotation Representation (b) Three Rotation Representation

Fig. 9. The roll angle error and the half cone angle error in Simulation 3

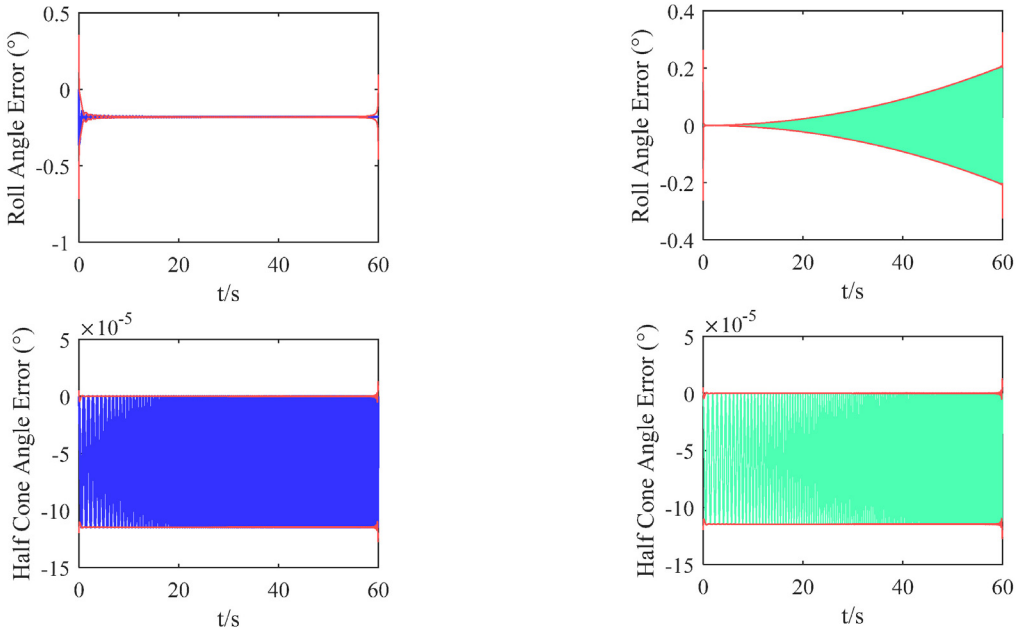

(a) Double Rotation Representation (b) Three Rotation Representation

Fig. 10. The roll angle error and the half cone angle error in Simulation 4

5 Conclusion

To address the disunification of flight movement and rotation representation, this paper proposes a double rotation representation for the angular motion, and the cone angles are defined between the reference frame and the body frame. Then, the paper derives the angular model as attitude updating algorithm based on the double rotation process in detail and use it for flight control, and provides an attitude algorithm with the rotation vector for navigation and the angle conversion between the double rotation representation and the three rotation representation. Simulations are made and results show that the double rotation representation can decouple the coning motion completely and has better accuracy than the three rotation representation. Moreover, the attitude algorithm with rotation vector has good resistance against the varying coning motion of varying cone speed and varying half cone angle but the non-commutative error still exists, and the condition with varying cone speed motion has a bigger effect than that with varying half cone angle. This work is helpful to understand the coning motion principle and the decouple attitude angles for control and navigation systems.

In the future work, the propagation principle of rotation vector error with the cone angles and the approach to restrain the vibrating error will be focused and investigated.

Acknowledgments

This study is financially supported in part by the Innovation Project of Beijing Municipal Education Commission under Grant KM201911232013, and in part by the Key Cultivation Project of Beijing Information Science and Technology University under Grant 5211910952.

Reference

[1] X. Hu, S. Yang, F. Xiong, G. Zhang, Stability of Spinning Missile with Homing Proportional Guidance law, Aerospace science and technology (71)(2017) 546-555.

[2] H. Zhao, Z. Su, Q. Li, F. Liu, N. Liu, Real-time Attitude Propagation Algorithm for High Spinning Flying Bodies, Measurement 177(2021) 109260.

[3] M. Xu, X. Bu, J. Yu, Z. He, Spinning Projectile's Attitude Measurement with LW Infrared Radiation under Sea-sky Background, Infrared Physics & Technology 90(2018) 214-220.

[4] K. Kim, T.G. Lee, Analysis of the Two-Frequency Coning Motion with SDINS, AIAA Guidance, Navigation, and Control Conference and Exhibit, 2001.

[5] J.E. Bortz, A New Mathematical Formulation for Strapdown Inertial Navigation, IEEE Transactions on Aerospace and Electronic Systems AES-7(1)(1971) 61-66.

[6] S. Theodoulis, Y. Morel, P. Wernert, Modelling and Stability Analysis of the 155 mm Spin-Stabilized Projectile Equipped with Steering Fins, International Journal of Modelling, Identification and Control 14(3)(2011) 189-204.

[7] R.B. Miller, A New Strapdown Attitude Algorithm, Journal of Guidance, Control and Dynamics 6(4)(1983) 287-291.

[8] M.B. Ignagni, Optimal Strapdown Attitude Integration Algorithms, Journal of Guidance, Control and Dynamics 13(2)(1990) 363-369.

[9] P.G. Savage, Coning Algorithm Design by Explicit Frequency Shaping, Journal of Guidance, Control and Dynamics 33(4)(2010) 1123-1132.

[10] L. Zhang, T. Zhang, M. Wang, J. Wang, Y. Li, A High-Order Coning Error Compensation Algorithm Under High Rate Maneuvering, IEEE Sensors Journal 20(1)(2020) 208-218.

[11] J.G. Mark, D.A. Tazartes, Tuning of Coning Algorithms to Gyro Data Frequency Response Characteristics, Journal of Guidance, Control and Dynamics 24(4)(2001) 641-646.

[12] Y. Wu, RodFIter: Attitude Reconstruction from Inertial Measurement by Functional Iteration, IEEE Transactions on Aerospace and Electronic Systems 54(5)(2018) 2131-2142.

[13] M. Wang, W. Wu, J. Wang, X. Pan, High-Order Attitude Compensation in Coning and Rotation Coexisting Environment, IEEE Transactions on Aerospace and Electronic Systems 51(2)(2015) 1178-1190.